

# Optically Excited Acoustic Vibrations in Quantum-Sized Monolayer-Protected Gold Clusters

Oleg Varnavski,<sup>†</sup> Guda Ramakrishna,<sup>\*</sup> Junhyung Kim,<sup>\*</sup> Dongil Lee,<sup>\*,§,\*</sup> and Theodore Goodson III<sup>†,\*</sup>

<sup>†</sup>Department of Chemistry, University of Michigan, Ann Arbor, Michigan 48109, <sup>‡</sup>Department of Chemistry, Western Michigan University, Kalamazoo, Michigan 49008, and

<sup>§</sup>Department of Chemistry, Yonsei University, Seoul 120-749, Korea

**ABSTRACT** We report a systematic investigation of the optically excited vibrations in monolayer-protected gold clusters capped with hexane thiolate as a function of the particle size in the range of 1.1–4 nm. The vibrations were excited and monitored in transient absorption experiments involving 50 fs light pulses. For small quantum-sized clusters ( $\leq 2.2$  nm), the frequency of these vibrations has been found to be independent of cluster size, while for larger clusters (3 and 4 nm), we did not observe detectable optically excited vibrations in this regime. Possible mechanisms of excitation and detection of the vibrations in nanoclusters in the course of the transient absorption are discussed. The results of the current investigation support a displacive excitation mechanism associated with the presence of finite optical energy gap in the quantum-sized nanoclusters. Observed vibrations provide a new valuable diagnostic tool for the investigations of quantum size effects and structural studies in metal nanoclusters.

**KEYWORDS:** gold clusters · thiolate · acoustic vibrations · quantum size effect

Metallc nanoscale materials with a size close to the Fermi wavelength of an electron have recently received a great amount of attention.<sup>1–4</sup> The research in this size regime has been sparked by their appeal in technological applications as well as the fundamental thrust of scientific understanding on the behavior of nanoscopic materials.<sup>1–8</sup> The acoustic response of these materials has great potential for their characterization<sup>9–16</sup> as well as for better understanding of fundamental aspects of quantum size effects.<sup>17</sup> Acoustic modes and their excitation characteristics in nanomaterials contain important information about structure, geometry, and interactions with the environment.<sup>9–17</sup> An unambiguous structural assignment of pristine clusters Au<sub>7</sub> and Au<sub>20</sub> in the gas phase, important for catalytical applications, has been done using vibrational spectroscopy.<sup>10</sup> It was also theoretically predicted that the nature of internal vibrational energy redistribution is a key factor in promoting reactivity of small gold clusters.<sup>11</sup> Vibration signature transfer in the THz range has been predicted be-

tween the polypeptide chain and gold nanocluster using molecular dynamics simulations.<sup>12,13</sup>

Among several metal clusters, gold clusters are the extensively investigated systems where the researchers observed a transition from bulk-like properties to molecular-like regimes, leading to quantum confinement effects.<sup>1,2,4,17,18</sup> Gold clusters comprising tens of atoms to several hundred atoms have been synthesized by stabilizing them with alkyl or aryl thiolates, and they are often referred to as monolayer-protected gold clusters (MPC).<sup>19</sup> The great complexity in the structural and electronic properties of these clusters becomes more apparent as their size decreases, leading to an intense interest and debate regarding the predictions of their properties.<sup>3,4,18</sup> MPCs<sup>19</sup> offer an exciting possibility to fabricate building blocks for potential applications in catalysis,<sup>5,6</sup> nonlinear optics<sup>7</sup> biolabeling,<sup>8</sup> memory, and electronic effects based on single electron charging processes.<sup>4,19</sup>

Coherently excited “breathing” vibrational mode for relatively large gold nanoparticles has been previously observed in a transient absorption signal as well as in Raman spectra.<sup>15,16</sup> The period of these vibrations was found to be from a few picoseconds to tens of picoseconds, and it was inversely proportional to the particle size. The impulsive heating of the particle lattice after short pulse laser excitation was suggested to be the origin of these vibrations.<sup>15,16,20,21</sup>

Quantum size effects lead to a transition from bulk-like (metallic) to a molecular-like behavior when the gold core size decreases down to the nanometer scale.<sup>1,4,17,18</sup> Quantization of energy as well as charge was observed for small size metal

\*Address correspondence to tgoodson@umich.edu, dongil@yonsei.ac.kr.

Received for review February 20, 2010 and accepted May 19, 2010.

Published online May 28, 2010. 10.1021/nn1003524

© 2010 American Chemical Society

clusters, and the electrochemical measurements have shown the size-dependent oxidation and reduction peaks.<sup>4,19</sup> Although there has been extensive research on the electrochemical and electron-transfer properties on the small sized MPCs, the acoustical properties in the quantum confinement regime remain unexplored.

In this paper, we have systematically investigated the optically excited vibrations in monolayer-protected gold clusters capped with hexane thiolate as a function of the particle size in the range of 1.1–4 nm. For small quantum-sized clusters, we found the frequency of these vibrations independent of cluster size, while for larger clusters (3 and 4 nm), we did not observe detectable optically excited vibrations in this regime. On the basis of these observations, we suggest the displacive excitation mechanism in quantum-sized clusters, which is qualitatively different from that in larger nanoparticles.

## RESULTS AND DISCUSSION

The organic-soluble nanoclusters were synthesized by using a modified Brust method<sup>22–25</sup> and solvent fractionated to reduce size dispersion. The isolated MPC core diameters were estimated from transmission electron microscopy (TEM) images which showed fairly narrow core size distributions (Figure 1):  $1.1 \pm 0.2$ ,  $1.7 \pm 0.2$ ,  $2.2 \pm 0.2$ ,  $3.0 \pm 0.3$ , and  $4.0 \pm 0.1$  nm.<sup>24</sup> On the basis of the TEM core diameters, the clusters were assigned, respectively, to  $\text{Au}_{25}(\text{SR})_{18}$ ,  $\text{Au}_{144}(\text{SR})_{60}$ ,  $\text{Au}_{309}(\text{SR})_{92}$ ,  $\text{Au}_{976}(\text{SR})_{187}$ , and  $\text{Au}_{2406}(\text{SR})_{326}$ , where SR is hexane thiolate, which were determined by mass spectrometry or modeling.<sup>25–27</sup>

The modified Brust method used in this work to prepare nanoclusters is essentially the same as the one in ref 25, where the structures and compositions of MPCs were thoroughly determined by a number of analytical techniques, including HR-TEM, small-angle X-ray scattering, XPS, thermogravimetric analysis (TGA), etc. The cluster compositions were determined by TGA and elemental analysis. The numbers of gold atoms and ligands are average ones and not perfectly accurate for relatively large clusters with core diameters  $\geq 2.2$  nm.<sup>25</sup> Recent studies provided the accurate compositions of small clusters.<sup>26–31</sup>

Shown in Figure 2 are the optical absorption spectra obtained for Au MPCs in hexane. Absorption spanning the visible to near-infrared region is seen for  $\text{Au}_{25}$  with distinct maxima around 675 and 410 nm and the ultraviolet region. Observed absorption spectra matched well with the previous reports and are ascribed to the quantized nature of the gold clusters.<sup>4,18,24,25,28,31</sup>

Time-resolved degenerate transient absorption studies have been carried out utilizing a pump–probe setup based on a cavity dumped Ti:sapphire laser system with a repetition rate of 38 kHz and a 20 fs pulse width.<sup>32,33</sup> This system possesses good noise character-

istics, allowing the sensitivity for relative transient absorption in the  $10^{-7}$  range at low pump pulse energies  $< 0.5$  nJ/pulse (less than 0.3 absorbed photons per MPC). We have investigated the degenerate transient absorption dynamics at 415 nm as a function of the gold cluster size. For larger size clusters exhibiting a surface plasmon resonance (SPR) band (3 and 4 nm), the pump–probe profile showed a rise-time feature followed by smooth exponential decay typical for larger size range.<sup>33,34</sup> A very different behavior in transient absorption dynamics and spectra has been observed for 2.2 nm clusters and smaller when compared to 3 nm ( $\text{Au}_{946}$ ) clusters (Figure 3). A subpicosecond oscillatory feature has been clearly detected in transient absorption for small gold clusters. Oscillatory features in the picosecond and subpicosecond time range have been found in transient absorption signals of semiconductors and semimetals<sup>14</sup> as well as in photoelectron spectroscopy and multiphoton ionization signals of very small pristine metal clusters.<sup>10,35,36</sup> Coherently excited “breathing” vibrational mode has been previously observed in transient absorption signal for relatively large gold nanoparticles.<sup>15,16</sup> The period of these vibrations was found in the order of picoseconds to tens of picoseconds and was inversely proportional to the particle size.<sup>15,16</sup> The excitation of these vibrations was assigned to the impulsive heating of the particle lattice after short pulse laser excitation.<sup>15</sup> This mechanism does not allow excitation of vibrations with a short period in the subpicosecond range (which is expected for small particles) due to finite picosecond electron–phonon coupling time ( $\sim 1$  ps).<sup>15,20,34</sup> Indeed, the oscillations in transient absorption experiments have not yet been reported for relatively small gold nanoparticles in the range of 1.1–8 nm.<sup>15</sup> In the present investigation, we did not observe any oscillatory features for 3 or 4 nm clusters. However, for small clusters of 1.1, 1.7, and 2.2 nm, the oscillatory structure has unexpectedly appeared (Figure 3). Multiple scans with different samples (including pure solvent), excitation and probe polarizations, power levels, and delay line scanning rates were performed to ensure the absence of the experimental artifacts. Oscillatory feature was clearly reproducible for all three small MPCs (1.1, 1.7, and 2.2 nm).

Analysis of the oscillations observed in the current experiments gave a period of  $\sim 450$  fs (2.2 THz). The observed frequency ( $\sim 74$   $\text{cm}^{-1}$ ) compares well to a low-frequency peak of vibrational density of states theoretically calculated for gold clusters<sup>12,37–39</sup> and is close the acoustic phonon density peak for the bulk gold.<sup>40</sup> Similar oscillatory feature has been recently reported for bound excited state of  $\text{Au}_5$  in a femtosecond photoelectron spectroscopy experiment<sup>35</sup> and has been ascribed to the vibrational wavepacket motion.<sup>35</sup> The theoretical simulation for  $\text{Au}_5$  predicted a period of 420 fs, while the experimental result gave a period of 315 fs,<sup>35</sup> both are quite close to the value that has been observed for

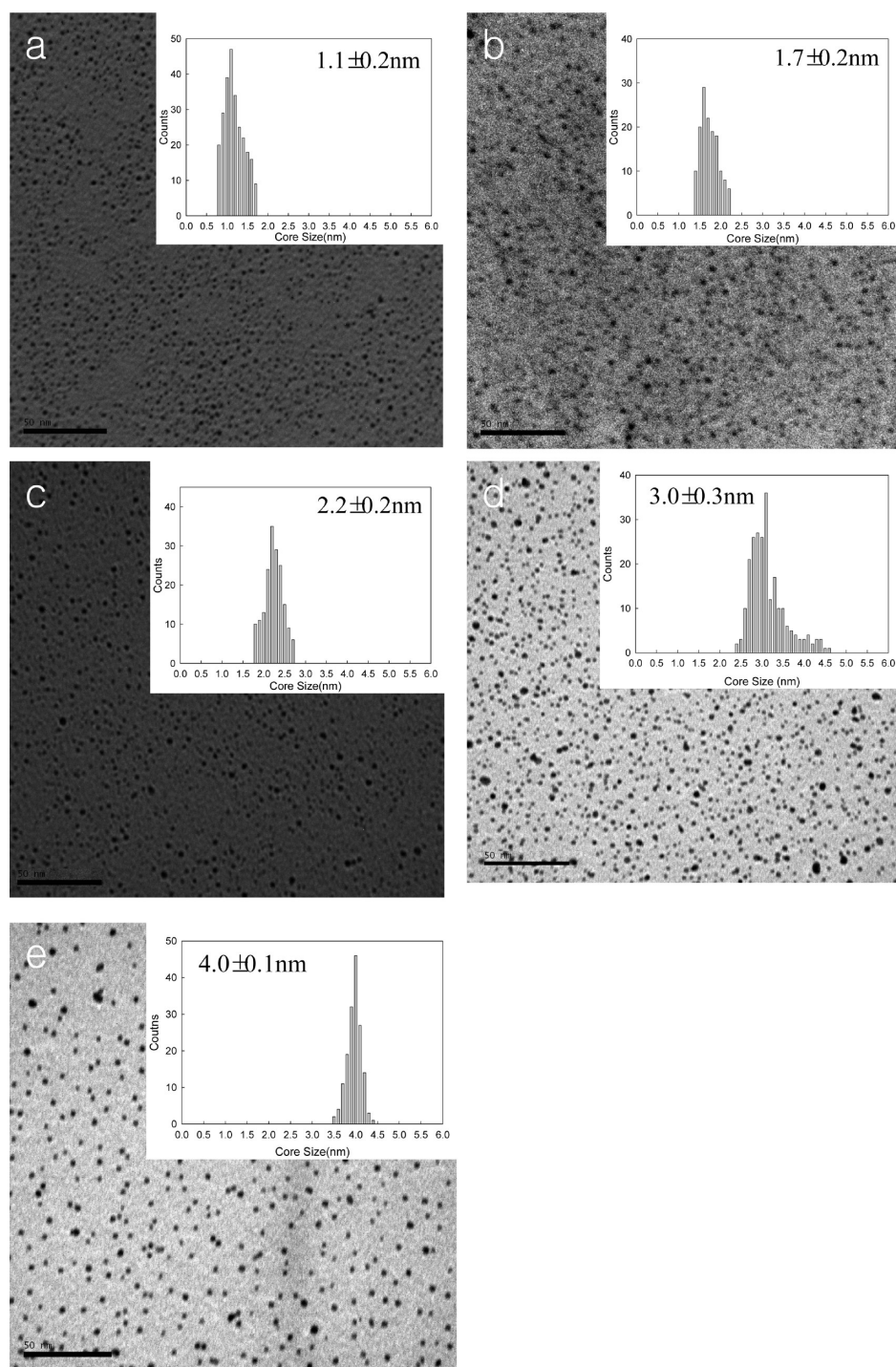


**Figure 1.** TEM images and corresponding histograms of the core diameters of hexane thiolate coated (a) Au<sub>25r</sub>, (b) Au<sub>144r</sub>, (c) Au<sub>309r</sub>, (d) Au<sub>976r</sub>, and (e) Au<sub>2406</sub> MPCs. Scale bar = 50 nm. TEM images were obtained with JEOL JEM-1230.

the present MPCs despite the size difference. Also, similar frequency ( $\sim 80 \text{ cm}^{-1}$ ) Fourier component was recently obtained from the transient absorption signal of Au<sub>25</sub>L<sub>18</sub><sup>-</sup> MPCs.<sup>41</sup>

As we mentioned above, impulsive heating mechanism cannot explain the excitation of relatively high frequency vibration in small clusters. In order to quantitatively analyze the oscillatory feature observed in transient absorption signal for small clusters and gain

better understanding of the possible mechanism, we have performed the multiexponential fits of the decay profiles and then investigated the residuals in detail. Analysis of the residuals to the best fit multiexponential decay (Figure 4) indicated a cosine-type oscillation (with max negative deviation at zero time, Figure 4, dashed line) in our experiment.

This is a characteristic feature for the displacive excitation mechanism of coherent phonons, which was ob-

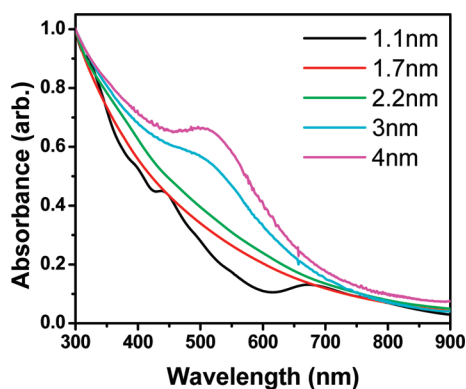


Figure 2. Optical absorption spectra of gold MPCs used in the experiment.

served in femtosecond transient absorption signals in semiconductors and semimetals for the phonons in the same frequency range<sup>14</sup> as well as in molecular systems.<sup>42</sup> After the impulsive excitation, the disturbed electronic system comes to equilibrium in a short time compared to the response time of the nuclear system, resulting in new equilibrium nuclear displacements.<sup>14</sup> The excitation of a superposition of vibrationally excited states in this area of potential surface generates the wavepacket motion.<sup>42</sup> These pump-induced coherent oscillations modulate the sample transmission through the modulation of the energy gap, thus making the oscillations for the probe pulse intensity a function of the delay time visible in the experiment. The change in transmission  $\Delta T(t)/T$  in semiclassical description can be written as<sup>14</sup>

$$\frac{\Delta T(t)}{T} = Mw_p \int_0^\infty G(t - \tau) \exp(-k_g \tau) d\tau + \\ Nw_p \frac{\omega_0^2}{\omega_0^2 + k_g^2 - 2\gamma k_g} \int_0^\infty G(t - \tau) \left\{ \exp(-k_g \tau) - \right. \\ \left. \exp(-\gamma \tau) \left[ \sqrt{1 + \frac{k_d^2}{\Omega^2}} \cos\left(\Omega \tau + \tan^{-1}\left(\frac{k_d}{\Omega}\right)\right) \right] \right\} d\tau \quad (1)$$

where  $G(t)$  is a pulse autocorrelation function,  $k_g$  is the excited state decay rate,  $w_p$  is the pump pulse energy per unit area,  $\omega_0$  is the angular frequency of the vibrational mode,  $\gamma$  is the damping constant for the vibrational mode,  $\Omega = \sqrt{\omega_0^2 - \gamma^2}$ ,  $k_d = k_g - \gamma$ , and  $N, M$  are constants related to the system dielectric function response to electronic excitation. It is seen from this expression that, in the case of relatively small oscillation damping and long excited state lifetime, the transient absorption oscillating component has cosine character with phase  $\Phi = \tan^{-1}(k_d/\Omega)$  approaching zero.<sup>14</sup> We have performed the least-squares fit analysis of the experimental residuals to the multiexponential fit to the decay curve (Figure 4). This analysis has provided us with the lifetime, frequency of the oscillations, and their phase with respect to cosine for different MPCs. For all three samples of 1.1, 1.7, and 2.2 nm, we have obtained about the same period of  $450 \pm 30$  fs and the phase  $\Phi$  scattered in the range of  $-25$  to  $+9^\circ$ , with no obvious correlation to the MPC size. This proves cosine-type oscillations typical for displacive origin of the vibrations, which have been observed in transient

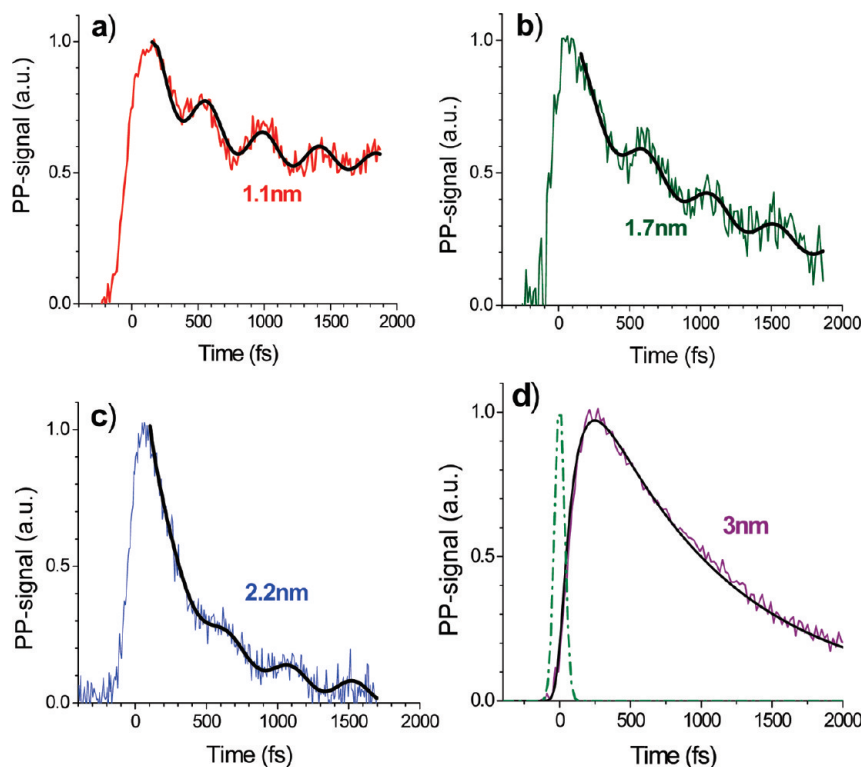


Figure 3. Transient absorption dynamics of gold MPCs of different sizes: (a) 1.1 nm, (b) 1.7 nm, (c) 2.2 nm, (d) 3 nm (solid lines – best fits; see text). Instrument response function is shown in (d) (dash-dot line).



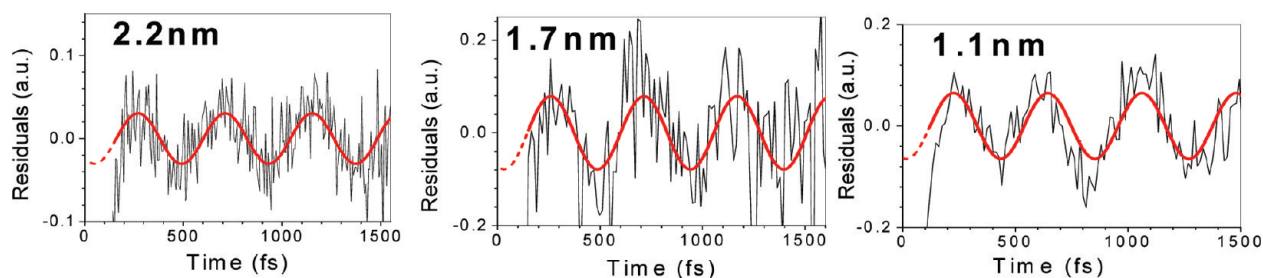


Figure 4. Analysis of the residuals to the best fit multiexponential decay of transient absorption signals. Best fit results to the residuals for different sizes are also shown (red solid lines). Dashed line shows the extension of the best fit function to zero time region.

absorption.<sup>14,42</sup> An important point is that the band gap is a prerequisite for these types of vibrations to be launched and detected by femtosecond pulses in the transient absorption experiment. It makes the observed oscillations a valuable indicator of the band gap opening.<sup>17</sup>

Another mechanism of the excitation of the vibrations in metal nanoparticles that could be considered for transient absorption experiment is the hot-electron pressure.<sup>43</sup> This mechanism is fast enough to be able to produce the correct phase of vibrations observed in our transient absorption experiments.<sup>43,44</sup> However, thermal pressure of electrons should initiate the breathing mode vibration of the entire gold core, the frequency of which is essentially size-dependent.<sup>43–45</sup> This is in disagreement with our observations (Figure 5). In addition, the oscillations in the transient absorption signal abruptly disappear for larger sizes of 3 and 4 nm (see Figure 3), which is also difficult to rationalize within the hot-electron pressure mechanism of vibration excitation.

Calculations of vibrational modes and density of vibrational states in gold clusters have been performed by different groups.<sup>37–39</sup> All of these papers report two peaks of phonon density of states (DOS) with a low-frequency peak located near 2 THz, which is close to the vibrational frequency detected in our experiment. The calculations also demonstrated the enhancement of the vibrational DOS at low frequencies for small clus-

ters as compared to that for bulk metal.<sup>9,12,37–40</sup> However, the vibrational frequency observed in the current experiment (2.2 THz) is closer to the main peak of the DOS for nanoclusters, not to the low-frequency tail mostly associated with the surface atoms.<sup>37–40</sup> Calculation of the fractional contributions to DOS from core and surface atoms for Au<sub>13</sub> also showed much stronger contribution of core gold atoms to the DOS peak near 2.2 THz as compared to those from the shell.<sup>38</sup> On the other hand, independence of size (Figure 5) may indicate the surface gold contribution. More experimental work and theoretical modeling is required to better spatially assign the observed vibrations. Excitation mechanism suggests that this mode should not lower the symmetry of the lattice, for example, A<sub>1</sub> breathing mode;<sup>14</sup> however, this is a local mode rather than a size-dependent breathing mode of the entire particle observed for larger nanoparticles. Polarization-sensitive measurements indicated a depolarized character of both transient absorption response and oscillatory feature (Figure 6). We found the oscillatory feature independent of the polarization (perpendicular or parallel to pump polarization) of the probe pulse. This observation supports high symmetry of the vibrational mode excited in the experiments.

In semiconductor particles, acoustic vibrational modes contribute to the transient absorption experiments because changes produced by the electronic ex-

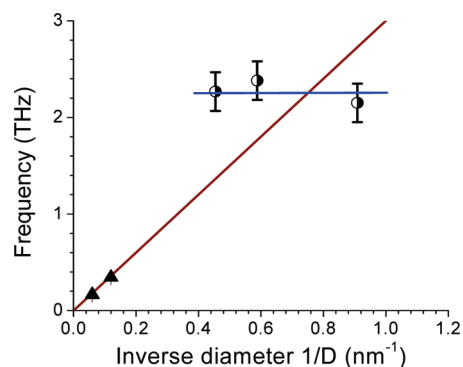


Figure 5. Acoustic vibration frequency size dependence (half-filled circles, this work). Solid triangles are frequencies of the “breathing” vibrational modes previously observed for larger gold particles.<sup>15,21</sup> Solid brown line is the classical elastic calculations for the elastic gold sphere.<sup>15,21,45</sup> Horizontal blue solid line is a guide to the eye.

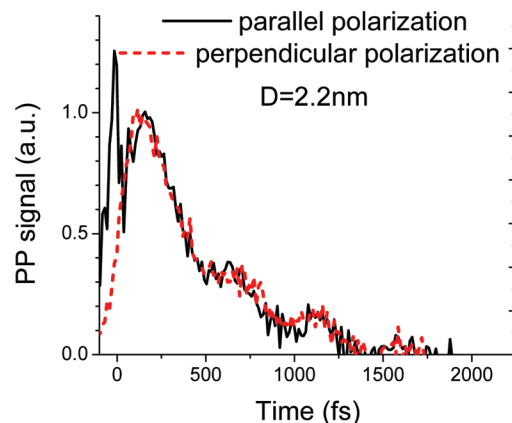


Figure 6. Transient absorption profiles for MPC (diameter 2.2 nm) with probe beam polarization perpendicular and parallel to pump polarization. Additional peak at zero position for parallel polarization is a coherent spike within the pulse time overlap area.

citation modify the band gap.<sup>14</sup> The system returning to the new equilibrium produces the oscillations around the recent position.<sup>14</sup> Importantly, this new electronic (density) configuration should be long-lived as compared to the period of oscillations in order for this optical excitation mechanism to work.<sup>14</sup> For the bulk metal and large nanoparticles, the intraband electron equilibration is too fast as compared to the vibrational period to support this mechanism.

However, if the energy gap emerges, the excited electron configuration lives much longer to maintain this new equilibrium position for many periods of vibrations as it takes place in semiconductors and molecular systems.<sup>14,42</sup> Hence, the appearance of the oscillations for small MPCs can be correlated to the emergence of an optical energy gap near the Fermi level.<sup>4,17</sup>

It is important to note that the frequency of the optically excited vibrations observed in this work does not appreciably vary with the MPCs size in the range of 1.1–2.2 nm (Figure 5, half-filled circles). This is very different from the situation in larger particles, where critically size-dependent breathing mode for the entire particle was excited in time-resolved optical experiments.<sup>15,16,20,21</sup> Figure 5 shows the vibrational frequency as a function of the inverse diameter. The

straight line indicates the frequency dependence for the elastic homogeneous sphere modes (Lamb model<sup>45</sup>). The frequencies observed for larger gold particles by other authors<sup>15,21</sup> (shown by triangles) agree with this model quite well.<sup>15,16,20,21</sup> Vibrations observed in this work deviate from both the elastic sphere model and the trend observed for larger particles well beyond the experimental error (indicated by error bars on Figure 5). This once again confirms that the vibrations observed in this work for quantum-sized gold MPCs are different in nature.

## CONCLUSION

In summary, we have observed optically excited vibrations in time-resolved experiments for gold MPCs in the size range of 1.1 nm (Au<sub>25</sub>) to 2.2 nm (Au<sub>309</sub>), where quantum size effects become essential. It has been found that both the origin and the excitation/detection mechanism of these vibrations are very different from those observed for larger gold nanoparticles.<sup>14,15</sup> Our results support a displacive excitation mechanism associated with the presence of a finite optical energy gap in these quantum-sized nanoclusters. These vibrational modes excited and detected in a wide size range of quantum-sized MPCs have a great potential for better MPC characterization.

## EXPERIMENTAL SECTION

**Sample Characterization.** Investigated gold clusters with hexane thiolates as capping agent have been synthesized by following a modified Brust's synthesis published elsewhere.<sup>22–25</sup> Transmission electron microscope (TEM) images of the synthesized gold clusters shown in Figure 1 provide the cluster diameters, and the number of gold atoms comprising the nanoparticles is obtained from the analysis. It can be observed from Figure 1 that all of the clusters have pretty good monodispersity, and the error bars in the sizes are fairly small. It has been shown that the stable cluster that has been previously mentioned to be Au<sub>38</sub>(SR)<sub>24</sub> is actually Au<sub>25</sub>(SR)<sub>16</sub>, and its detailed structure has been determined.<sup>23–26,29–31</sup> Also, more accurate composition structure for Au<sub>144</sub>(SR)<sub>60</sub> has been recently suggested.<sup>27,28</sup>

**Optical Absorption Measurements.** Optical absorption measurements on the investigated samples have been carried out with an Agilent (model #8341) spectrophotometer.

**Transient Absorption Measurements.** Time-resolved degenerate transient absorption studies have been carried out utilizing a cavity dumped Ti:sapphire laser system, which was spectrally centered at 830 nm with a repetition rate of 38 kHz and 20 fs pulse width.<sup>32</sup> The fundamental is passed through a nonlinear BBO crystal, and the second harmonic is generated, which is then directed to the pump–probe section. The degenerate pump–probe setup was a transient absorption configuration of a three-pulse photon echo setup based on the cavity dumped laser system previously described in detail.<sup>32,46</sup> This transient absorption system possessed very good noise characteristics, allowing the sensitivity for relative transient absorption in the 10<sup>–7</sup> range at very low pump pulse energy <0.5 nJ/pulse (less than 0.3 absorbed photons per MPC). This is very important as the transient absorption signal for small clusters is relatively weak due to the absence of surface plasmon resonance. Low pump pulse energy of ~0.5 nJ is also important to measure the true electron system cooling profile in larger clusters possessing surface plasmon resonance as this profile is excitation-intensity-dependent in this case.<sup>21,34</sup> The probe beam of the same wave-

length is passed through an optical delay line and the lens, and then it is overlapped with the pump beam in the sample cell and is detected by the photodiode. Modulated probe signal was measured with the use of a lock-in amplifier synchronized to optical chopper in the pump beam and recorded as a function of delay line on a PC. The width of the instrument response function was ~65 fs.<sup>32,46</sup>

**Acknowledgment.** Financial support of the National Science Foundation is gratefully acknowledged (T.G.). D.L. thanks the World Class University (R32-2008-000-10217-0) and the Priority Research Centers (2009-0093823) programs through the National Research Foundation of Korea for financial support.

## REFERENCES AND NOTES

- de Heer, W. A. The Physics of Simple Metal Clusters: Experimental Aspects and Simple Models. *Rev. Mod. Phys.* **1993**, *65*, 611–676.
- Walter, M.; Akola, J.; Lopez-Acevedo, O.; Jadzinsky, P. D.; Calero, G.; Ackerson, C. J.; Whetten, R. L.; Grönbeck, H.; Häkkinen, H. A Unified View of Ligand-Protected Gold Clusters as Superatom Complexes. *Proc. Natl. Acad. Sci. U.S.A.* **2008**, *105*, 9157–9162.
- Jadzinsky, P. D.; Calero, G.; Ackerson, C. J.; Bushnell, D. A.; Kornberg, R. D. Structure of a Thiol Monolayer-Protected Gold Nanoparticle at 1.1 Å Resolution. *Science* **2007**, *318*, 430–433.
- Chen, S.; Ingram, R. S.; Hostetler, M. J.; Pietron, J. J.; Murray, R. W.; Schaaff, T. G.; Khoury, J. T.; Alvarez, M. M.; Whetten, R. L. Gold Nanoelectrodes of Varied Size: Transition to Molecule-like Charging. *Science* **1998**, *280*, 2098–2101.
- Turner, M.; Golovko, V. B.; Vaughan, O. P. H.; Abdulkin, P.; Berenguer-Murcia, A.; Tikhov, M. S.; Johnson, B. F. G.; Lambert, R. M. Selective Oxidation with Dioxxygen by Gold Nanoparticle Catalysts Derived from 55-Atom Clusters. *Nature* **2008**, *454*, 981–984.

6. Valden, M.; Lai, X.; Goldman, D. W. Onset of Catalytic Activity of Gold Clusters on Titania with the Appearance of Nonmetallic Properties. *Science* **1998**, *281*, 1647–1650.
7. Ramakrishna, G.; Varnavski, O.; Kim, J.; Lee, D.; Goodson, T. Quantum Sized Gold Clusters as Efficient Two-Photon Absorbers. *J. Am. Chem. Soc.* **2008**, *130*, 5032–5033.
8. Hainfeld, J. F. A Small Gold-Conjugated Antibody Label: Improved Resolution for Electron Microscopy. *Science* **1987**, *236*, 450–453.
9. Kara, A.; Rahman, T. S. Vibrational Properties of Metallic Nanocrystals. *Phys. Rev. Lett.* **1998**, *81*, 1453–1456.
10. Gruene, P.; Rayner, D. M.; Redlich, B.; Van der Meer, A. F. G.; Lyon, J. T.; Meijer, G.; Fielicke, A. Structures of Neutral Au<sub>7</sub>, Au<sub>19</sub>, and Au<sub>20</sub> Clusters in the Gas Phase. *Science* **2008**, *321*, 674–676.
11. Mitric, R.; Bürgel, C.; Bonacic-Kourtecky, V. Reactivity-Promoting Criterion Based on Internal Vibrational Energy Redistribution. *Proc. Natl. Acad. Sci. U.S.A.* **2007**, *104*, 10314–10317.
12. Miao, L.; Seminario, J. M. Molecular Dynamics Simulations of the Vibrational Signature Transfer from a Glycine Peptide Chain to Nanosized Gold Clusters. *J. Phys. Chem. C* **2007**, *111*, 8366–8371.
13. Miao, L.; Seminario, J. M. Molecular Dynamics Simulations of Signal Transmission through a Glycine Peptide Chain. *J. Chem. Phys.* **2007**, *127*, 134708.
14. Zeiger, H. J.; Vidal, J.; Cheng, T. K.; Ippen, E. P.; Dresselhaus, G.; Dresselhaus, M. J. Theory for Displacive Excitation of Coherent Phonons. *Phys. Rev. B* **1992**, *45*, 768–778.
15. Hartland, G. V. Coherent Excitation of Vibrational Modes in Metallic Nanoparticles. *Annu. Rev. Phys. Chem.* **2006**, *57*, 403–430.
16. Portales, H.; Saviot, L.; Duval, E.; Fujii, M.; Hayashi, S.; Del Fatti, N.; Vallee, F. Resonant Raman Scattering by Breathing Modes of Metal Nanoparticles. *J. Chem. Phys.* **2001**, *115*, 3444–3447.
17. Varnavski, O.; Ramakrishna, G.; Kim, J.; Lee, D.; Goodson, T. Critical Size for the Observation of Quantum Confinement in Optically Excited Gold Clusters. *J. Am. Chem. Soc.* **2010**, *132*, 16–17.
18. Wyrwas, R. B.; Alvarez, M. M.; Khoury, J. T.; Price, R. C.; Schaaff, T. G.; Whetten, R. L. The Colours of Nanometric Gold. *Eur. Phys. J. D* **2007**, *43*, 91–95.
19. Templeton, A. C.; Wuelfing, W. P.; Murray, R. W. Monolayer-Protected Cluster Molecules. *Acc. Chem. Res.* **2000**, *33*, 27–36.
20. Voisin, C.; Del Fatti, N.; Christoflos, D.; Vallee, F. Ultrafast Electron Dynamics and Optical Nonlinearities in Metal Nanoparticles. *J. Phys. Chem. B* **2001**, *105*, 2264–2280.
21. Hodak, J. H.; Henglein, A.; Hartland, G. V. Size Dependent Properties of Au Particles: Coherent Excitation and Dephasing of Acoustic Vibrational Modes. *J. Chem. Phys.* **1999**, *111*, 8613–8621.
22. Brust, M.; Walker, M.; Bethel, D.; Schiffrin, D. J.; Whyman, R. Synthesis of Thiol-Derivatized Gold Nanoparticles in a Two-Phase Liquid–Liquid System. *J. Chem. Soc., Chem. Commun.* **1994**, 801–802.
23. Kim, J.; Lee, D. Electron Hopping Dynamics in Au<sub>38</sub> Nanoparticle Langmuir Monolayers at the Air/Water Interface. *J. Am. Chem. Soc.* **2006**, *128*, 4518–4519.
24. Kim, J.; Lee, D. Size-Controlled Interparticle Charge Transfer between TiO<sub>2</sub> and Quantized Capacitors. *J. Am. Chem. Soc.* **2007**, *129*, 7706–7707.
25. Hostetler, M. J.; Wingate, J. E.; Zhong, C.-J.; Harris, J. E.; Vachet, R. W.; Clark, M. R.; Londono, J. D.; Green, S. J.; Stokes, J. J.; Wignall, G. D.; Glish, G. L.; Porter, M. D.; Evans, N. D.; Murray, R. W. Alkanethiolate Gold Cluster Molecules with Core Diameters from 1.5 to 5.2 nm: Core and Monolayer Properties as a Function of Core Size. *Langmuir* **1998**, *14*, 17–30.
26. Tracy, J. B.; Crowe, M. C.; Parker, J. F.; Hampe, O.; Fields-Zinna, C. A.; Dass, A.; Murray, R. W. Electrospray Ionization Mass Spectrometry of Uniform and Mixed Monolayer Nanoparticles: Au<sub>25</sub>[S(CH<sub>2</sub>)<sub>2</sub>Ph]<sub>18</sub> and Au<sub>25</sub>[S(CH<sub>2</sub>)<sub>2</sub>Ph]<sub>18-x</sub>(SR)<sub>x</sub>. *J. Am. Chem. Soc.* **2007**, *129*, 16209–16215.
27. Lopez-Acevedo, O.; Akola, J.; Whetten, R. L.; Grönbeck, H.; Häkkinen, H. Structure and Bonding in Ubiquitous Icosahedral Metallic Gold Cluster Au<sub>144</sub>(SR)<sub>60</sub>. *J. Phys. Chem. C* **2009**, *113*, 5035–5038.
28. Qian, H.; Jin, R. Controlling Nanoparticles with Atomic Precision: The Case of Au<sub>144</sub>(SCH<sub>2</sub>CH<sub>2</sub>Ph)<sub>60</sub>. *Nano Lett.* **2009**, *9*, 4083–4087.
29. Heaven, M. W.; Dass, A.; White, P. S.; Holt, K. M.; Murray, R. W. Crystal Structure of the Gold Nanoparticle [N(C<sub>8</sub>H<sub>17</sub>)<sub>4</sub>][Au<sub>25</sub>(SCH<sub>2</sub>CH<sub>2</sub>Ph)<sub>18</sub>]. *J. Am. Chem. Soc.* **2008**, *130*, 3754–3755.
30. Akola, J.; Walter, M.; Whetten, R. L.; Häkkinen, H.; Grönbeck, H. On the Structure of Thiolate-Protected Au<sub>25</sub>. *J. Am. Chem. Soc.* **2008**, *130*, 3756–3757.
31. Zhu, M.; Aikens, C. M.; Hollander, F. J.; Schatz, G. C.; Jin, R. Correlating the Crystal Structure of a Thiol-Protected Au<sub>25</sub> Cluster and Optical Properties. *J. Am. Chem. Soc.* **2008**, *130*, 5883–5885.
32. Varnavski, O.; Sukhominova, L.; Twieg, R.; Goodson III, T. Ultrafast Exciton Dynamics in a Branched Molecule Investigated by Time-Resolved Fluorescence, Transient Absorption, and Three-Pulse Photon Echo Peak Shift Measurements. *J. Phys. Chem. B* **2004**, *108*, 10484–10492.
33. Varnavski, O. P.; Mohamed, M. B.; El-Sayed, M. A.; Goodson III, T. Femtosecond Excitation Dynamics in Gold Nanospheres and Nanorods. *Phys. Rev. B* **2005**, *72*, 235–405.
34. Link, S.; El-Sayed, M. A. Shape and Size Dependence of Radiative, Non-radiative and Photothermal Properties of Gold Nanocrystals. *Int. Rev. Phys. Chem.* **2000**, *19*, 409–453.
35. Stanzel, J.; Burmeister, F.; Neeb, M.; Eberhardt, W.; Mitric, R.; Bürgel, C.; Bonacic-Kourtecky, V. Size-Dependent Dynamics in Excited States of Gold Clusters: From Oscillatory Motion to Photoinduced Melting. *J. Chem. Phys.* **2007**, *127*, 164312.
36. Bescos, B.; Lang, B.; Weiner, J.; Weiss, V.; Wiedenmann, E.; Gerber, G. Real-Time Observation of Ultrafast Ionization and Fragmentation of Mercury Clusters. *Eur. Phys. J. D* **1999**, *9*, 399–403.
37. Calvo, S. R.; Balbuena, P. B. Molecular Dynamics Studies of Phonon Spectra in Mono- and Bimetallic Nanoclusters. *Surf. Sci.* **2005**, *581*, 213–224.
38. Lee, W.-L.; Ju, S.-P.; Sun, S.-J.; Weng, M.-H. Dynamical Behaviour of 7-1 Gold Nanowire under Different Axial Tensile Strains. *Nanotechnology* **2006**, *17*, 3253–3258.
39. Sun, D. Y.; Gong, X. G.; Wang, X.-Q. Soft and Hard Shells in Metallic Nanocrystals. *Phys. Rev. B* **2001**, *63*, 193412.
40. Lynn, J. W.; Smith, H. G.; Nicklow, R. M. Lattice Dynamics of Gold. *Phys. Rev. B* **1973**, *8*, 3493–3499.
41. Miller, S. A.; Wormik, J. M.; Parker, J. F.; Murray, R. W.; Moran, A. M. Femtosecond Relaxation Dynamics of Au<sub>25</sub>L<sub>18</sub><sup>-</sup> Monolayer-Protected Clusters. *J. Phys. Chem. C* **2009**, *113*, 9440–9444.
42. Walmsley, I. A.; Wise, F. W.; Tang, C. L. On the Difference between Quantum Beats in Impulsive Stimulated Raman Scattering and Resonance Raman Scattering. *Chem. Phys. Lett.* **1989**, *154*, 315–320.
43. Perner, M.; Gresillon, S.; März, J.; von Plessen, G.; Feldmann, J.; Porstendorfer, J.; Berg, K.-J.; Berg, G. Observation of Hot-Electron Pressure in the Vibration Dynamics of Metal Nanoparticles. *Phys. Rev. Lett.* **2000**, *85*, 792–795.
44. Voisin, C.; Del Fatti, N.; Christoflos, D.; Valle'e, F. Time-Resolved Investigation of the Vibrational Dynamics of Metal Nanoparticles. *Appl. Surf. Sci.* **2000**, *164*, 131–139.
45. Lamb, H. On the Vibrations of an Elastic Sphere. *Proc. London Math. Soc.* **1882**, *13*, 189–212.
46. Varnavski, O.; Yan, X.; Mongin, O.; Blanchard-Desce, M.; Goodson, T., III. Strongly Interacting Organic Conjugated Dendrimers with Enhanced Two-Photon Absorption. *J. Phys. Chem. C* **2007**, *111*, 149–162.